side in Fig. 4, and also the lower two rows in Fig. 4).

The energy state, both magnetic and kinetic, of a magnetohydrodynamic dynamo in a rotating spherical shell has two local minima, namely, the dynamo system can alternately take a high- or low-energy state. More specifically, the system flip-flops in an irregular fashion between a high- and a low-energy state. A reversal occurs only in a high-energy state and only if the high-energy state is maintained for a certain period. More interestingly, there appears a rather gradual growth phase of the quadrupole mode before a reversal, and a reversal occurs when the magnitude of the quadrupole mode exceeds that of the dipole at the outer boundary. Note, however, that when an observer measures the quadrupole component on Earth's surface, this is not the case because the quadrupole mode amplitude decreases much faster than that of the dipole as the radial distance increases.

The most important discovery of these simulations is the generation of trans-equatorial flows in a spherical system that makes the convection pattern vulnerable and the whole system marginally stable. Reversal of the dipole magnetic field arises with a good correlation with the generation of trans-equatorial flows. We remind here that Sarson and Jone (*12*) and Sarson (*13*) have made an argument on the importance of nonaxisymmetric poloidal flow on the reversal.

The necessary conditions for the occurrence of a dipole reversal obtained in our model are the following: (i) The system is in a high-energy state, (ii) the high-energy state lasts for a certain period, (iii) the quadrupole mode is on the average in a growing phase, and (iv) the magnitude of the quadrupole mode exceeds that of the dipole mode on the outer boundary. The last two conditions are consistent with the suggested correlations between field strengths and reversals (*14*). Although the parameter region of the real Earth is far from the present one, we believe that the core mechanism of the dipole reversal must be a universal one, as is often the case for most phenomena in nature, and that the elementary reversal mechanism could be the generation of the north-south asymmetric flow. This is because the flow pattern is the only direct agency related to the magnetic field pattern. Furthermore, other simulation runs have disclosed that the energy state always stays in a high-energy state for larger Rayleigh numbers. In Earth's case, the Rayleigh number is much higher than those of our simulation examples. Thus, it is quite likely that reversal can take place in the real Earth.

References

1. H. K. Moffatt, *Magnetic Field Generation in Electrically Conducting Fluids* (Cambridge Univ. Press, Cambridge, 1978).
2. P. H. Roberts, A. M. Soward, *Annu. Rev. Fluid Mech.* **24**, 459 (1992).
3. P. H. Roberts, G. A. Glatzmaier, *Rev. Mod. Phys.* **72**, 1081 (2000).
4. J. A. Jacobs, *Reversals of the Earth's Magnetic Field* (Cambridge Univ. Press, Cambridge, ed. 2, 1994).
5. R. T. Merrill, M. W. McElhinny, P. L. McFadden, *The Magnetic Field of the Earth: Paleomagnetism, the Core, and the Deep Mantle* (Academic Press, San Diego, CA, 1996).
6. G. A. Glatzmaier, P. H. Roberts, *Nature* **377**, 203 (1995).
7. A. Kageyama, T. Sato, The Complexity Simulation Group, *Phys. Plasmas* **2**, 1421 (1995).
8. _____, *Phys. Rev. E* **55**, 4617 (1997).
9. A. Kageyama, M. M. Ochi, T. Sato, *Phys. Rev. Lett.* **82**, 5409 (1999).
10. G. A. Glatzmaier, R. S. Coe, L. Hongre, P. H. Roberts, *Nature* **401**, 885 (1999).
11. R. S. Coe, L. Hongre, G. A. Glatzmaier, *Philos. Trans. R. Soc. London Ser. A* **358**, 1141 (2000).
12. G. R. Sarson, C. A. Jones, *Phys. Earth Planet. Inter.* **111**, 3 (1999).
13. G. R. Sarson, *Philos. Trans. R. Soc. London Ser. A* **358**, 921 (2000).
14. A. Cox, *J. Geophys. Res.* **73**, 3247 (1968).

9 October 2001; accepted 4 February 2002

Antarctic Krill Under Sea Ice: Elevated Abundance in a Narrow Band Just South of Ice Edge

Andrew S. Brierley,[1]*† Paul G. Fernandes,[2] Mark A. Brandon,[3] Frederick Armstrong,[2] Nicholas W. Millard,[4] Steven D. McPhail,[4] Peter Stevenson,[4] Miles Pebody,[4] James Perrett,[4] Mark Squires,[4] Douglas G. Bone,[1] Gwyn Griffiths[4]

We surveyed Antarctic krill (*Euphausia superba*) under sea ice using the autonomous underwater vehicle *Autosub-2*. Krill were concentrated within a band under ice between 1 and 13 kilometers south of the ice edge. Within this band, krill densities were fivefold greater than that of open water. The under-ice environment has long been considered an important habitat for krill, but sampling difficulties have previously prevented direct observations under ice over the scale necessary for robust krill density estimation. *Autosub-2* enabled us to make continuous high-resolution measurements of krill density under ice reaching 27 kilometers beyond the ice edge.

Antarctic krill (*Euphausia superba*) is a key species in the Southern Ocean and depends on sea-ice algae for food at some stages of its life cycle (*1*). Interannual changes in the recruitment success of krill have been linked to oscillations in sea-ice extent, and krill abundance may decline following successive winters of reduced ice coverage (*2*). Reductions in krill abundance have major consequences throughout the Southern Ocean ecosystem (*3*) and affect commercial fisheries (*4*), and it is essential to understand interactions of krill with sea ice. In summer, the marginal ice zone (MIZ), where melting sea ice is broken into floes by waves and swell, is a region of elevated primary productivity (*5*). Phytoplankton blooms develop in the upper water column that is stabilized by melt-water, and krill may feed on these blooms. It has long been presumed that krill abundance is elevated along sea-ice edges because some krill-eating whales aggregate there (*6*). However, although krill swarms have been seen in open water between sea-ice floes (*7*) and discrete spot-measurements have detected krill under ice (*8–11*), there is a paucity of quantitative information on the mesoscale distribution and abundance of krill beneath ice because of difficulties associated with sampling there. Limitations with conventional methods have prevented continuous observations beneath ice over the scale necessary to assess krill robustly: ice-breaking ships disrupt the sea-ice habitat, and scuba divers and remotely operated vehicles suffer restricted operating ranges. Evidence for krill–sea ice links thus remains largely circumstantial (*2*). Here, we report acoustic survey data gathered along replicated line-transects by the autonomous underwater vehicle (AUV) *Autosub-2* (*12*) during its first missions beneath sea ice. These data enable krill density and distribu-

[1]British Antarctic Survey, High Cross, Madingley Road, Cambridge CB3 0ET, UK. [2]Fisheries Research Services (FRS) Marine Laboratory Aberdeen, Post Office Box 101, Victoria Road, Aberdeen, AB11 9DB, UK. [3]The Open University, Department of Earth Sciences, Walton Hall, Milton Keynes, MK7 6AA, UK. [4]Southampton Oceanography Centre, Empress Dock, Southampton SO14 3ZH, UK.

*To whom correspondence should be addressed. E-mail: andrew.brierley@st-andrews.ac.uk

†Present address: Gatty Marine Laboratory, University of St. Andrews, Fife, KY16 8LB, UK.

tion under ice to be assessed directly.

We conducted acoustic surveys of seven pairs of parallel transects spanning the edge of the MIZ at approximately 63° south in the Weddell Sea between 27 January and 8 February 2001 (*13*). We sought to test the null hypothesis that the presence of sea-ice cover had no effect on the density (g m^{-2}) of Antarctic krill in underlying waters. Open waters to the north of the sea-ice edge were surveyed by the research vessel RRS *James Clark Ross* using a 38 and 120 kHz scientific echosounder (*13*). Ice-covered waters to the south of the sea-ice edge were surveyed by *Autosub-2* with the same type of echosounder adapted for autonomous deployment (*14*). *Autosub-2* surveyed more than 210 km of transect under ice. Both the ship and AUV surveyed an overlapping central section of most transects to enable between-platform comparisons (*13*). The echosounder on the AUV was directed upward to the sea surface, whereas the ship's echosounder was directed downward; krill target strength is the same in both dorsal and ventral aspects (*15*). Analyses elsewhere have shown that krill do not avoid RRS *James Clark Ross* significantly (*16*). There was no systematic difference between the krill-detection capabilities of the ship or the AUV, and the two data sets were directly comparable. Echoes from *Euphausia superba* (Fig. 1) were identified by using differences in echo intensity (*13*, *17*) and swarm morphology. Krill were caught by net from the ship in open water to determine length-frequency distributions and to confirm the identity of acoustic targets. Krill were caught in all nets fished through targets that had the acoustic appearance of krill.

Within the region we surveyed, krill density was significantly higher under sea ice than in open water (*t* test, $t = 2.283$, $n = 37$, $P = 0.015$) (*13*). Mean weighted krill density under ice was 61.6 g m^{-2} (SEM 5.1 g m^{-2}) but was only 20.6 g m^{-2} (SEM 2.4 g m^{-2}) in open water. There was no significant difference between the mean krill densities detected by the ship or the AUV along the sections of transects surveyed by both (paired sample *t* test, $t = 0.720$, $n = 9$, $P = 0.492$, power = 0.70). The mean open-water krill density is typical of oceanic areas, whereas the density under ice is of the order expected for productive shelf-break regions (*18*). The estimate of density under sea ice is probably conservative because of the association of krill, particularly juveniles, with crevices within the ice (*8*) that we were unable to sample acoustically. The acoustic dead-zone (*19*) extending approximately 1 m beneath the ice-water interface also prevented sampling there.

Regression analysis was used to investigate relationships between the spatial distribution of krill along-transect and distance from the sea-ice edge. A modified normal function fitted the data well and suggested that krill density was elevated significantly in a band extending from 1 to 13 km south of the sea-ice edge [analysis of variance (ANOVA) $n = 19$, $F = 19.383$, $P < 0.0001$, $r^2 = 0.847$; Fig. 2A]. Within this band, modeled krill density was 83.4 g m^{-2} compared with 16.8 g m^{-2} outside. A survey of sea-ice concentration (*13*, *20*) was conducted perpendicular to the sea-ice edge before the first *Autosub-2* mission (Fig. 2B). Krill density increased southward from the point where ice concentration was greater than about 40%. The MIZ is a dynamic and heterogeneous environment (*21*), but the consistent pattern of krill distribution relative to the local sea-ice edge repeated along all transects indicates that the zone just south of the sea-ice edge is a habitat of particular importance for krill. Whaling data implicated the sea-ice edge as an area important for krill (*7*) but gave no indication of the distance into the ice that krill extended. Our continuous survey data show that abundance declines rapidly after 13 km.

Krill swarms were associated significantly with the presence of keels and other topographic features (Fig. 1). Of the 194 swarms detected, 164 occurred less than 185 m horizontally from sea-ice projections extending more than 2.5 m deeper than the immediate mean sea-ice depth (binomial $P \ll 0.001$). Scuba diver observations of krill beneath ice have suggested that abundance is elevated in the vicinity of pressure ridges or other complex under-ice topography

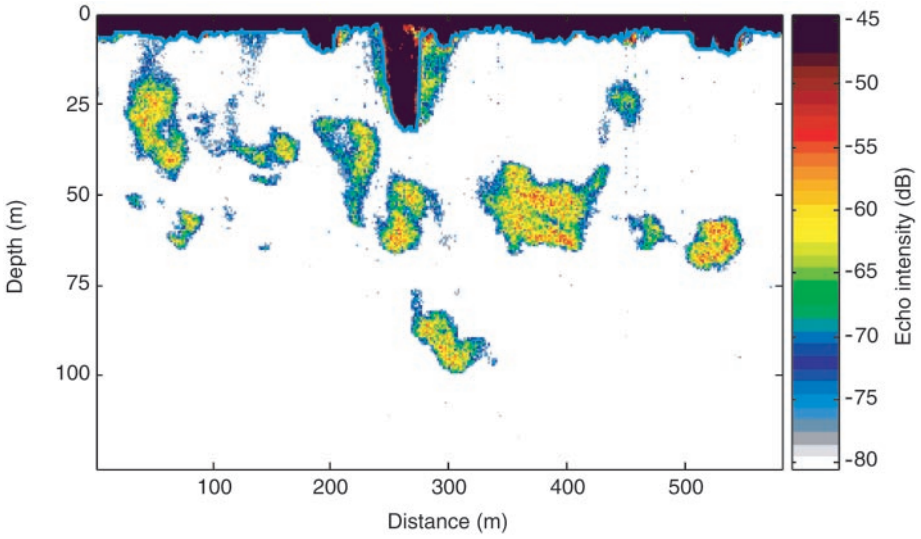

Fig. 1. A 38-kHz echogram shows krill swarms under sea ice (15:30 local time, 27 January). The blue line marks the ice-water interface. Color scale shows echo intensity from −45 dB (approximately 4430 krill m^{-3}) to −80 dB (1.4 krill m^{-3}). The features immediately adjacent to the iceberg (top center) are side-lobe echoes that were not evaluated as krill.

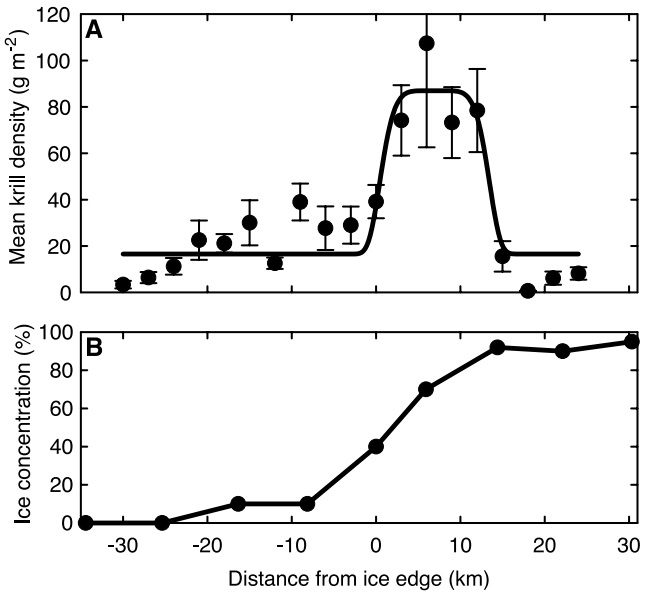

Fig. 2. Krill distribution relative to the sea-ice edge and ice concentration. (**A**) Krill density by distance (in 3 km bins, positive is under ice) from the local sea-ice edge. The line is the highly significant regression function; error bars are ±1 SEM. (**B**) Sea-ice concentration.

(*8*, *22*). Krill distributions are, however, notoriously patchy (*23*), and point estimates of abundance are unlikely to be representative of the regional mean. Previous studies comparing krill densities in open and ice-covered waters based on extrapolations from point samples reach contrary conclusions, highlighting shortcomings of these approaches. Netting surveys have suggested both that krill density is elevated under sea ice compared with that in open water (*10*) and that there is no difference in density (*24*). Spot acoustic observations in the same area found highest krill densities in open water most distant from the sea-ice edge (*8*). Ship-based continuous line-transect acoustic surveys have been used to estimate krill density in open water north of the sea-ice edge. A survey in the Weddell Sea (*9*) found a mean krill density near the ice edge of 23.2 g m^{-2}, which is similar to that detected in open water here. Echosounders on ice-strengthened research vessels have detected krill swarms along transects through ice-covered seas, but it has not been possible to determine krill density accurately from data collected from ships moving through ice because of interference caused by ice-breaking noise (*25*). The unique sampling capabilities of *Autosub-2* and echosounder combined have enabled us to describe a link between krill density and sea-ice cover directly and quantitatively.

Our data suggest krill are coupled tightly to a zone just inside the sea-ice edge. This coupling may be an example of risk balancing (*1*, *24*), with krill locating actively at a compromise point that is both near to high concentrations of food (the ice edge) and that provides refuge from predators (air breathers that cannot dive through ice). Whatever the cause, the fact that krill do not appear to be distributed evenly under ice may mean that any reductions in ice area, perhaps following climate change (*26*), do not lead to directly proportional reductions in krill biomass. Any krill reductions may instead be in proportion to the reduction of ice-edge length. The purported 25% reduction in ice area in the 1960s (*27*) equates to a 9% reduction in edge length: consequences for krill may not have been as grave as has been implied.

References and Notes

1. L. B. Quetin, R. M. Ross, T. K. Frazer, K. L. Haberman, *Antarct. Res. Ser.* **70**, 357 (1996).
2. V. Loeb *et al.*, *Nature* **387**, 897 (1997).
3. K. Reid, J. P. Croxall, *Proc. R. Soc. London B Biol. Sci.* **268**, 377 (2001).
4. I. Everson, G. Parkes, K.-H. Kock, I. L. Boyd, *J. Appl. Ecol.* **36**, 591 (1999).
5. K. R. Arrigo, D. Worthen, A. Schnell, M. P. Lizotte, *J. Geophys. Res.* **103**, 15587 (1998).
6. T. Ichii, *Proc. National Institute for Polar Research (NIPR) Symp. Polar Biol.* **3**, 36 (1990).
7. J. W. S. Marr, *Discovery Rep.* **32**, 33 (1962).
8. K. L. Daly, M. C. Macaulay, *Deep-Sea Res. I* **35**, 21 (1988).
9. M. Godlewska, *Polar Biol.* **13**, 507 (1993).
10. V. Siegel, A. Skibowski, U. Harm, *Polar Biol.* **12**, 15 (1992).
11. I. Sprong, P. H. Schalk, *Polar Biol.* **12**, 261 (1992).
12. N. W. Millard *et al.*, *J. Soc. Underwater Technol.* **23**, 7 (1998).
13. Details of survey design, acoustic methods, and data analysis are available on *Science* Online at www.sciencemag.org/cgi/content/full/295/5561/1890/DC1
14. P. G. Fernandes, A. S. Brierley, "Using an autonomous underwater vehicle as a platform for mesoscale acoustic sampling in marine environments," *ICES CM 1999/M:01* [International Council for the Explorations of the Sea (ICES), Copenhagen, 1999].
15. D. E. McGehee, R. L. O'Driscoll, L. V. Martin Traykovski, *Deep-Sea Res. II* **45**, 1273 (1998).
16. A. S. Brierley *et al.*, *Fisheries Res.*, in press.
17. J. L. Watkins, A. S. Brierley, *WG-EMM-97/46* [Commission for the Conservation of Antarctic Marine Living Resources (CCAMLR), Hobart, 1997].
18. A. S. Brierley, J. L. Watkins, C. Goss, M. T. Wilkinson, I. Everson, *CCAMLR Sci.* **6**, 47 (1999).
19. E. Ona, R. B. Mitson, *ICES J. Mar. Sci.* **53**, 677 (1996).
20. A. P. Worby, *Observing Antarctic Sea Ice* (ASPeCt, Hobart, CD-ROM, 1999).
21. D. R. Turner, N. J. P. Owens, *Deep-Sea Res. II* **42**, 907 (1995).
22. V. Siegel, B. Bergström, J.-O. Strömberg, P. H. Schalk, *Polar Biol.* **10**, 549 (1990).
23. A. W. A. Murray, *ICES J. Mar. Sci.* **53**, 415 (1996).
24. K. L. Daly, M. C. Macaulay, *Mar. Ecol. Prog. Ser.* **79**, 37 (1991).
25. A. S. Brierley, J. L. Watkins, *Can. J. Fish. Aquat. Sci.* **57** (suppl. 3), 24 (2000).
26. D. G. Vaughan, G. J. Marshall, W. M. Connolley, J. C. King, R. Mulvaney, *Science* **293**, 1777 (2001).
27. W. K. de la Mare, *Nature* **389**, 57 (1997).

28. We thank Captain Elliot, officers and crew of RRS *James Clark Ross* cruise 58, and C. Drew, P. Lens, M. Preston, M. Robjant, and R. Woodd-Walker for assistance at sea. We are grateful to D. Demer for advice on echosounder configuration, D. McGehee for target strength information, E. Murphy for comments on our draft manuscript, and A. Shanks for statistical advice. This research was funded by the UK Natural Environment Research Council.

30 November 2001; accepted 30 January 2002

The Role of Endosymbiotic *Wolbachia* Bacteria in the Pathogenesis of River Blindness

Amélie v. Saint André,[1] Nathan M. Blackwell,[1,2] Laurie R. Hall,[1] Achim Hoerauf,[3] Norbert W. Brattig,[3] Lars Volkmann,[3] Mark J. Taylor,[4] Louise Ford,[4] Amy G. Hise,[1] Jonathan H. Lass,[2] Eugenia Diaconu,[2] Eric Pearlman[1,2]*

Parasitic filarial nematodes infect more than 200 million individuals worldwide, causing debilitating inflammatory diseases such as river blindness and lymphatic filariasis. Using a murine model for river blindness in which soluble extracts of filarial nematodes were injected into the corneal stroma, we demonstrated that the predominant inflammatory response in the cornea was due to species of endosymbiotic *Wolbachia* bacteria. In addition, the inflammatory response induced by these bacteria was dependent on expression of functional Toll-like receptor 4 (TLR4) on host cells.

Wolbachia bacteria are essential symbionts of the major pathogenic filarial nematode parasites of humans, including *Brugia malayi* and *Wuchereria bancrofti*, which cause lymphatic filariasis, and *Onchocerca volvulus*, which causes river blindness (*1*). *Wolbachia* spp. are abundant in all developmental stages of filarial nematodes, including the hypodermis and reproductive tissue of adult parasites (*1*). In contrast to their relatives in arthropods, *Wolbachia* spp. in filarial nematodes appear to have evolved as an essential endosymbiont. Antibiotic therapy in humans and experimental filarial infection has shown that embryogenesis is completely dependent on the presence of *Wolbachia* (*2*, *3*). Furthermore, parasites recovered from tetracycline-treated animals are stunted, and larval development is attenuated (*2*). In *O. volvulus*–infected individuals, adult worms survive for up to 14 years in subcutaneous nodules in the human host and release millions of microfilariae over this time (*4*). Microfilariae migrate through the skin and can enter the posterior and anterior regions of the eye. While alive, the microfilariae appear to cause little or no inflammation; however, when they die, either by natural attrition or after chemotherapy, the host response to degenerating worms can result in ocular inflammation that causes progressive loss of vision and ultimately leads to blindness (*4*, *5*).

Following the discovery of endosymbiont-derived endotoxin-like activity of *B. malayi* and *O. volvulus* (*6*, *7*), we sought to determine the role of *Wolbachia* in the

[1]Division of Geographic Medicine, [2]Department of Ophthalmology, University Hospitals of Cleveland and Case Western Reserve University, Cleveland, OH 44106, USA. [3]Bernhard Nocht Institute for Tropical Medicine, 20359 Hamburg, Germany. [4]Liverpool School of Tropical Medicine, Pembroke Place, Liverpool L3 5QA, UK.

*To whom correspondence should be addressed. E-mail: exp2@po.cwru.edu